TROPICAL LIFE SCIENCES RESEARCH

Antioxidant Metabolites from *Justicia gendarussa* Fractions based on UHPLC-Q-Orbitrap-HRMS Metabolomics and Density Functional Theory Approach

Authors:
Faizal Maulana, Waras Nurcholis, Trivadila and Irmanida Batubara*

***Correspondence:** ime@apps.ipb.ac.id

Received: 3 May 2024; **Accepted**: 21 April 2026; **Early view**: 26 August 2026
To cite this article: Maulana F, Nurcholis W, Trivadila and Batubara I. (in press). Antioxidant metabolites from *Justicia gendarussa* fractions based on UHPLC-Q-Orbitrap-HRMS metabolomics and density functional theory approach. *Tropical Life Sciences Research*.

Highlights

- *Justicia gendarussa* demonstrates significant potential as a promising natural source of active antioxidants.

- Metabolomics successfully profiled and identified active compounds with chemometrics, such as PCA, heatmaps, and OPLS-DA, classified metabolites by polarity, identifying six active antioxidant compounds and isolable unknowns in the ethyl acetate fraction.

- Density functional theory (DFT) validated the theoretical determination of the most effective antioxidant metabolites within the plant.

EARLY VIEW

Antioxidant Metabolites from *Justicia gendarussa* Fractions based on UHPLC-Q-Orbitrap-HRMS Metabolomics and Density Functional Theory Approach

[1]Faizal Maulana, [3,4]Waras Nurcholis, [2,3]Trivadila and [2,3]Irmanida Batubara*

[1]Magister study program in chemistry, Department of Chemistry, Faculty of Mathematics and Natural Sciences, IPB University, Bogor, 16680, West Java, Indonesia
[2]Department of Chemistry, Faculty of Mathematics and Natural Sciences, IPB University, Bogor, 16680, West Java, Indonesia
[3]Tropical Biopharmaca Research Center, IPB University. Jl. Taman Kencana No.3, Bogor, 16128, West Java, Indonesia
[4]Department of Biochemistry, Faculty of Mathematics and Natural Sciences, IPB University, Bogor, 16680, West Java, Indonesia

*Corresponding author: ime@apps.ipb.ac.id

Running head: Antioxidant Metabolites from *Justicia gendarussa*

Received: 3 May 2024; **Accepted**: 21 April 2026; **Early view**: 26 August 2026
To cite this article: Maulana F, Nurcholis W, Trivadila and Batubara I. (in press). Antioxidant metabolites from *Justicia gendarussa* fractions based on UHPLC-Q-Orbitrap-HRMS metabolomics and density functional theory approach. *Tropical Life Sciences Research*.

Abstract: The herb *Justicia gendarussa*, known as gendarussa, has the potential as an antioxidant. A previous study has identified that ethanol extract from *J. gendarussa* has the highest antioxidant activity. The study profiled the metabolites of *n*-hexane, ethyl acetate, *n*-butanol, and water fractions of its ethanol extract using ultrahigh performance liquid chromatography-high resolution mass spectrometry (UHPLC-Q-Orbitrap HRMS). The antioxidant capacities of metabolites were determined using 2,2-diphenyl-1-picrylhydrazyl (DPPH), 2,2′-azinobis-(3-ethylenebenzothiazoline)-6-sulfonic acid (ABTS), ferric ion reducing antioxidant power (FRAP), and cupric reducing antioxidant capacity (CUPRAC) method combined with chemometric technique. Finally, a computational density functional theory (DFT) study was carried out to ensure the ability of the active compounds as an antioxidant. The results showed that the highest antioxidant capacity of the DPPH method was on the *n*-

butanol fraction of 40.5 *μ*mol (trolox equivalent) TE/g dry fraction, while the ABTS, FRAP, and CUPRAC methods were on the ethyl acetate fraction with antioxidant capacity were 69.0, 189, and 624 *μ*mol TE/g dry fraction. Principal component analysis (PCA) and heatmap succeeded in classifying the metabolites in *J. gendarussa* fraction based on polarity. There were 37 and 21 identified metabolites in positive and negative ionization, respectively. Using orthogonal partial least square-discriminant analysis (OPLS-DA), the predictive active antioxidant metabolites were gendarusin A, justridusamide A, sesamol, 6-{[(Benzyloxy)carbonyl]amino}-6-deoxy-1,2-O-isopropylidene-α-D-glucofuranose, methyl 2-[cyclohex-2-en-1-yl(hydroxy)methyl]-3-hydroxy-4-(2-hydroxyethyl)-3-methyl-5-oxoprolinate, and 3,4-Dihydroxy-6-(N-ethylamino) benzamide. In addition, 14 unknown metabolites in the ethyl acetate fraction were predicted to be active antioxidants, which can be isolated for further research to obtain new metabolites. Density functional theory (DFT) proves that 6-{[(Benzyloxy)carbonyl]amino}-6-deoxy-1,2-O-isopropylidene-α-D-glucofuranose and gendarusin A have a smaller energy gap than trolox as a standard, indicating it has a better antioxidant ability. Therefore, those two compounds are the best antioxidant compounds. Additional tests *in vitro* or *in vivo* research on the isolation compounds results need to be carried out to prove the research results further.

Keywords: DFT, Gendarussa, Heatmap, OPLS-DA, PCA.

INTRODUCTION

Justicia gendarussa (Acanthaceae), commonly known as gendarussa, is a prominent medicinal plant found across several Asian countries, including Indonesia, India, Malaysia, and Sri Lanka (Ratih et al. 2019). It was selected for this study due to its diverse and unique ethnopharmacological profile; it serves as a traditional male contraceptive in Papua, Indonesia, while in India, it is used to treat conditions including headaches, bronchitis, arthritis, jaundice, otalgia, digestive disorders, fever, cancer, and for UV protection (Putri et al. 2020). This therapeutic versatility is driven by a rich composition of secondary metabolites, including phenolics, alkaloids, steroids, and terpenoids (Widodo et al. 2019). Notably, the plant contains specific flavonoids, including gendarusins A–E, with gendarusin A as the major metabolite (Kumar et al. 2018; Ratih et al. 2019). Other bioactive constituents identified include the alkaloid group brazoides A–D (Souza et al. 2016; Zhang et al. 2021a), the steroid stigmasterol (Uddin et al. 2011), and terpenoids such as (+) and (-)-genpenterpene A (Zhang et al. 2021b). These metabolites provide a distinct chemical scaffold for the development of potential antioxidants.

The significance of identifying potent antioxidants lies in their ability to mitigate the damage caused by oxidative stress (Chaudhary 2015). Such oxidative damage is fundamentally linked to the progression of various chronic diseases, including neurodegenerative disorders, diabetes mellitus, cardiovascular diseases, rheumatoid arthritis, cataracts, respiratory diseases, and various types of cancer (Di Meo & Venditti, 2020). These pathologies are driven by reactive oxygen species (ROS) produced by cellular metabolism, including hydrogen peroxide (H_2O_2), hydroxyl radicals (OH•), superoxide anion radicals (O_2^-•), and peroxyl radicals (ROO•) (Çalişkan et al. 2021). While previous research has confirmed the antioxidant capacity of *J. gendarussa* leaf ethanol extracts (Kuber 2021) and identified high DPPH scavenging activity in the ethyl acetate fraction of the aerial parts (Zhang et al. 2021a), significant knowledge gaps remain. Specifically, no study has yet reported the antioxidant potential across a different polarity like n-hexane, ethyl acetate, n-butanol, and water fractions using an integrated metabolomics and density functional theory approach.

To address these gaps, this study utilizes metabolomics combined with orthogonal partial least squares-discriminant analysis (OPLS-DA) to correlate biological activity with chemical profiles. This methodology has identified active markers in other plants, such as rosmarinic acid in *Orthosiphon aristatus* (Maulana et al. 2022) and epicatechin/epigallocatechin in *Xylocarpus granatum* (Heryanto et al. 2023). Furthermore, we employ computational chemistry through density functional theory (DFT) to validate the molecular reactivity and thermodynamic properties of these compounds (Kaddouri 2020). This approach provides a comprehensive understanding of antioxidant mechanisms through gap energy (ΔE) analysis (Ramadhan 2021). By integrating metabolomics and DFT, this research offers a more rapid and cost-effective alternative to traditional bioassay-guided isolation (Maulana et al. 2022). Consequently, this study aims to identify and theoretically evaluate the active antioxidant compounds in specific fractions of *J. gendarussa*.

MATERIALS AND METHODS

Cultivation and Sample Preparation

Plant cultivation takes place in Biopharmaca Cultivation Conservation Unit, Cikabayan Gardens Block C, IPB Dramaga Bogor Campus, Indonesia, located at 6°3'49"S and 106°42'57" E, at 240 m above sea level. The cultivation for all treatment plants received 100 kg/ha of P_2O_5 fertilizer, 150 kg/ha of KCl, 270 kg/ha nitrogen fertilizer, and 20 tons/ha of cow manure. The fertilizer is mixed and distributed in polybags (10 × 15 cm) around plants grown for one month, then transferred to larger polybags (30 × 30 cm). The leaves and stems of *J. gendarussa*, which had been fertilized for four months, were harvested at age of 4 month. In

addition, the sample's dried weight was determined by drying it in an oven at 45°C for 2 × 24 hours.

Preparation of Fractions

Sample of 10 g *J. gendarussa* aerial parts (leaves and stems) were extracted with 100 mL of ethanol p.a. in a ratio of 1:10 for 24 hours in a dark place at room temperature. Multilevel fractionation was carried out using *n*-hexane, ethyl acetate*, n*-butanol, and water as the solvent with a volume ratio of 1:2 for each solvent. A sample of 1 g of the extract was dissolved in 25 mL of distilled water and then put into a 500 mL separating funnel. The solution was added with 50 mL of solvent. The layer of solvent was separated into bottle. The resulting *n*-hexane, ethyl acetate, *n*-butanol and water fractions were then evaporated using a rotary evaporator. Fractionation with each solvent was repeated three times.

Antioxidant Capacity

The DPPH method refers to Batubara *et al.* (2020), a 100 *µ*L of the sample solution of *J. gendarussa* fractions and 100 *µ*L of 125 *µ*M DPPH was added to a 96-well clear polystyrene microplate. Mixed solution was incubated for 30 minutes in a dark place at room temperature. The absorbance was measured with a microplate nano spectrophotometer at 515 nm wavelength.

The ABTS method refers to Nurcholis *et al.* (2022), a 20 *µ*L of the fractions sample and 180 *µ*L of ABTS reagent was added on a 96-well clear polystyrene microplate. Then, the mixed solution was incubated for 6 minutes. The absorbance of the mixed solution was measured using a microplate nano spectrophotometer at 734 nm wavelength.

The FRAP method refers to Batubara *et al.* (2020), a 10 *µ*L samples of *J. gendarussa* fractions and 145 *µ*L of FRAP was added into a 96-well clear polystyrene microplate and then incubated in a dark place at room temperature for 4 minutes. The absorbance of the sample was read at 593 nm wavelength using a microplate nano spectrophotometer.

The CUPRAC method refers to Nurcholis *et al.* (2022), a 50 *µ*L of the fractions sample was added to 50 *µ*L of 10^{-2} M $CuCl_2$ solution, 50 *µ*L of NH_4Ac buffer 1 M with pH 7, and 50 *µ*L of 7.5×10^{-3} M neocuproin on a microplate. Then, the mixed solution was incubated in a dark room for 30 minutes at room temperature. Then, the absorbance of the solution was calculated at 450 nm using a microplate nano spectrophotometer. All method used calibration curves with standard trolox solution with various concentrations. The results are equivalent to *µ*mol trolox equivalent per gram dry weight (*µ*mol TE/g dry fraction weight) (Nurcholis *et al.* 2022).

Metabolite Identification Using UHPLC-Q-Orbitrap HRMS

Metabolites were identified using the Vanquish UHPLC-Q Exactive Plus Orbitrap-High Resolution Mass Spectrometer. A 5 mg sample was dissolved in 1 mL of LC-MS grade methanol, then sonicated for 10 minutes and filtered through a 0.2 μm filter membrane. Separation chromatography was performed using an AccucoreTM Vanquish C18+ column (1.5 μm, 120 Å, 2.1 × 100 mm). Water and 0.1% formic acid were used as the A mobile phase, while acetonitrile and 0.1% formic acid were used as the B mobile phase. The gradient system used is 0 – 1 minute (5% B), 1- 18 minutes (5- 45 % B), 18 – 30 minutes (45 – 95% B), 30 – 33 minutes (95% B), and 33 – 35 minutes (5% B). The column temperature is 30°C. Electrospray ionization (ESI) with a spray voltage of 3800 volts (ESI+) and 3200 volts (ESI-) were used as the ionization source. The mass analyzer was a quadrupole orbitrap (tandem MS/MS), m/z range of 100-1500 Da. The ionization energies were set at 18, 35 and 53 eV. An injection volume of 2 μL.

Identification of metabolites was carried out using the data in the form of RAW processed with MzMine software. The data were loaded, and feature detection was performed to identify relevant peaks. Parameters for polarity were set to both positive and negative ion modes, with a retention time range of 0 – 35.0 minutes, and a noise level threshold of 10^4. The ADAP chromatogram builder was used, with a minimum intensity threshold of 10^6 and an m/z tolerance of 0.05 m/z or 5 ppm. Chromatogram deconvolution was applied with baseline cut-off algorithm with baseline level 10^6 and minimum peak height 3×10^6. Followed by gap filling for the m/z and retention time with m/z tolerance of 5 ppm, and grouping of isotopic peaks with retention time tolerance of 0.25 min. All samples were aligned, and metabolites identification was performed using an inhouse metabolite database. Putative identification of metabolites was carried out by comparing the MS and MS-MS spectra against an in-house database and the MetFrag webserver.

Density Functional Theory (DFT) Studies

Method refers to Rammohan *et al.* (2020), the molecular structure of active antioxidant compounds was optimized and calculated using the DFT B3LYP basis sets 6-31G calculation method with GaussView. The parameters of the molecules reactivity as antioxidants are the highest occupied molecular orbital (HOMO) and lowest unoccupied molecular orbital (LUMO) energyvalues. This energy value is obtained by calculating the system total energy, known as single point energy. Single point energy calculation is carried out on the optimal compound structure. The parameters used are gap energy (ΔE), ionization energy (I), and electron affinity (A).

Data and Multivariate Analysis

Analysis of antioxidant capacity data for this study used Minitab software with One Way ANOVA analysis, which was expressed by a p-value < 0.05. Next, Tukey's post hoc test was carried out for tests that were significantly different. Analysis was carried out to find out the treatment that had the most influence on all the tests that had been carried out. All tests were visualized using GraphPad Prism software.

Before carrying out multivariate analysis for UHPLC-Q-Orbitrap HRMS data, pre-processing of the chromatogram with correlation optimized warping (COW) was carried out using The Unscrambler X. Determination of the reference chromatogram is carried out using the similarity index formula and the highest similarity index chromatogram is used as the reference chromatogram. The search for optimal segment length and slack was set with a ratio of 5:1. The ratio starts from 5:1 to 100:20. The highest chromatogram similarity index was selected as data for multivariate analysis. Multivariate PCA, heatmap, and OPLS-DA analyses were performed using the MetaboAnalyst webserver.

To ensure data quality and comparability, a specific preprocessing workflow was implemented: Normalization by Sum was applied to correct variations between samples, followed by Data Transformation using Log Transformation (log 10) to normalize the data distribution. Finally, Data Scaling was performed using Mean Centering to emphasize the biological variance between the different fractions (*n*-hexane, ethyl acetate, *n*-butanol, and water).

Unsupervised PCA was used to visualize the chemical distribution based on fraction polarity. Subsequently, supervised OPLS-DA was utilized to correlate the chemical profiles with antioxidant activity. Models were validated based on R^2X, R^2Y, and Q^2 values, where a $Q^2 > 0.5$ indicated high predictive reliability. Active antioxidant candidates were selected based on three strict criteria: a Variable Importance in Projection (VIP) score > 1.0, a p-value < 0.05, and a Fold Change (FC) > 2.0. Additionally, a hierarchical clustering heatmap was generated using Pearson distance and Ward’s linkage to visualize the relative concentrations of identified metabolites across the fractions.

RESULTS AND DISCUSSION

Antioxidant Capacity

Antioxidant capacity was calculated using trolox as the standard curve for all methods. All of the one-way ANOVA tests of *J. gendarussa*’s aerial part fractions using the DPPH, ABTS,

FRAP, and CUPRAC methods had significantly different results (Figure 1). The highest antioxidant capacity for the DPPH method was found in the *n*-butanol fraction at 40.5 *µ*mol (trolox equivalent) TE/g dry fraction. However, it was not significantly different from the ethyl acetate fraction. Then, the highest antioxidant capacity of the ABTS and FRAP methods was found in the ethyl acetate fraction at 69.0 and 189 *µ*mol TE/g dry fraction, respectively. Finally, the highest antioxidant capacity of the CUPRAC method was found in the ethyl acetate fraction at 624 *µ*mol TE/g dry fraction. However, it was not significantly different from the *n*-butanol fraction.

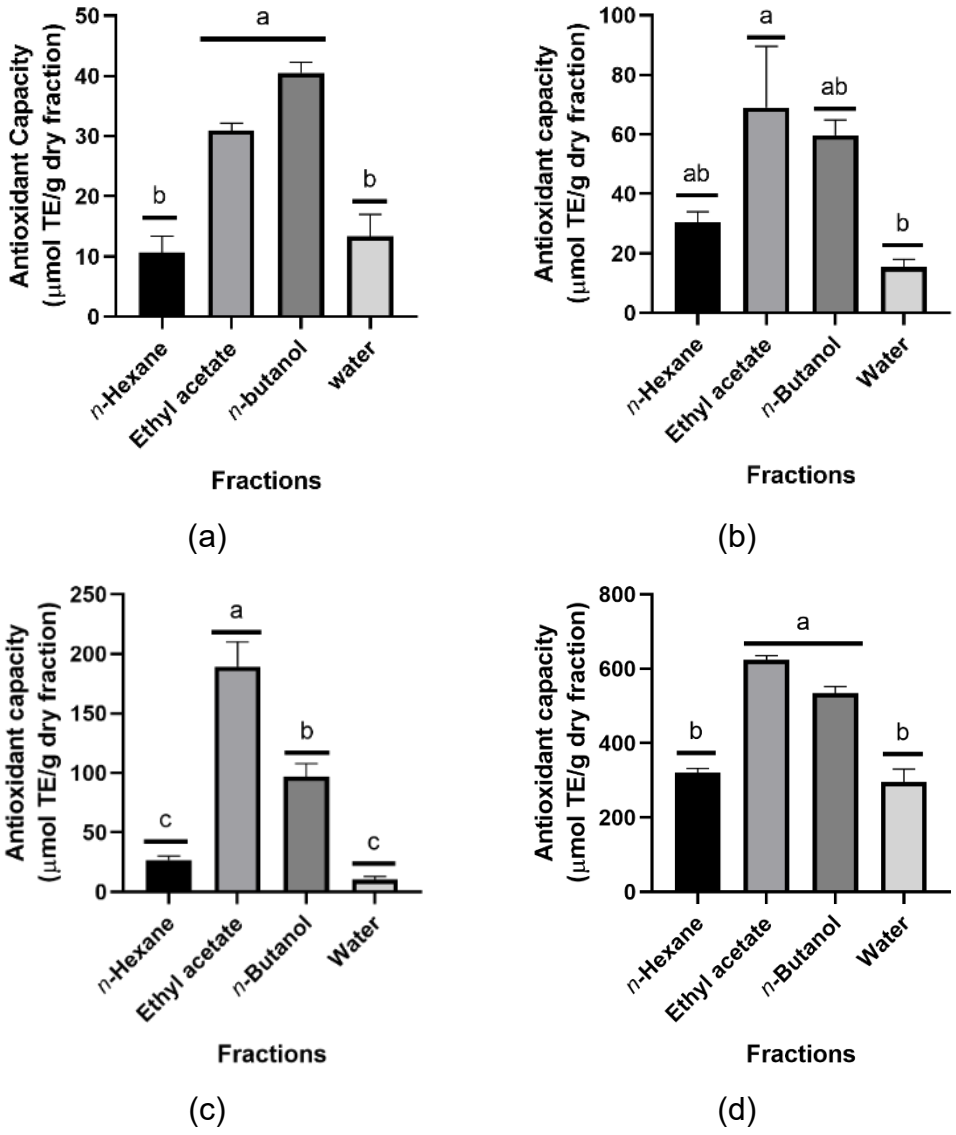

Figure 1. Antioxidant capacity of *J. gendarussa*'s aerial parts fraction (a) DPPH (b) ABTS (c) FRAP and (d) CUPRAC method. Each value is presented as the mean ± standard error of mean (SEM). The mean value in each column marked with a different letter is significantly different at $p < 0.05$ or the 95% confidence level.

It was concluded that active antioxidant compounds are possible in the ethyl acetate or *n*-butanol fraction. These results were compared with research by Zhang *et al.* (2021a), fractionating the aerial parts of *J. gendarussa* using petroleum ether and ethyl acetate, it was found that compounds from the ethyl acetate fraction had the highest antioxidant activity against DPPH with an IC_{50} value of 28.61 μM and the quercetin control was 18.56 μM. The antioxidant values with four different methods, namely DPPH, ABTS, FRAP, and CUPRAC, have different results, which can be caused by the uniqueness of each reaction principal method and the content of secondary metabolites contained that have been separated based on different polarities (Sadeer *et al.* 2020).

Metabolites Identified Using UHPLC-Q-Orbitrap HRMS

Positive and negative ionization modes of chromatograms were produced from *J. gendarussa*'s aerial parts fractions (Figures 2a and 2b). There were 37 and 21 metabolites identified in positive and negative ionization mode, respectively. The distribution of metabolites that have been identified can be seen in the Venn diagram (Figures 2c and 2d), with detailed metabolite identification results in Tables 1 and 2. The results of metabolite identification using UHPLC-Q-Orbitrap HRMS are putative. Fragmentation is carried out for metabolites with a high-intensity mass spectrum.

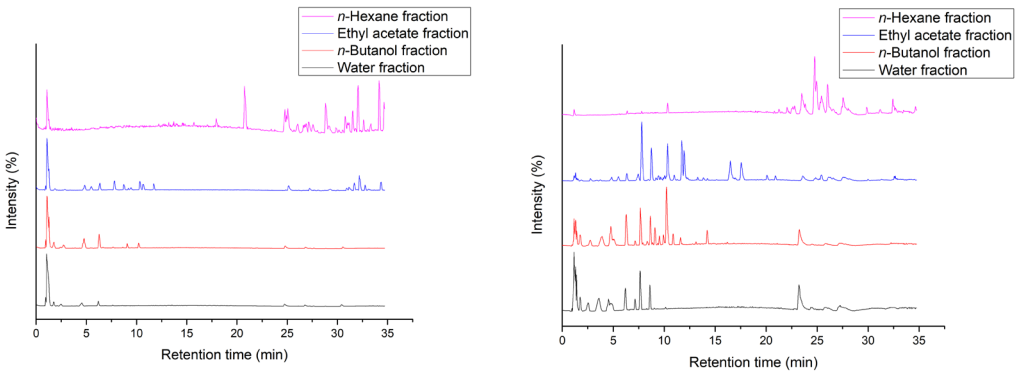

(a) (b)

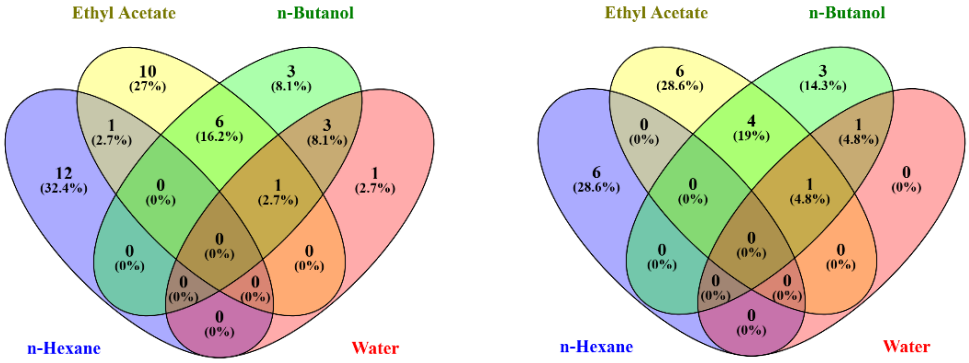

(c) (d)

Figure 2. Fraction chromatogram (a) positive ionization mode (b) negative ionization mode. Venn diagram of identified compounds (a) positive ionization mode (b) negative ionization mode.

Table 1: Identified metabolites with positive ionization in *J. gendarussa*'s aerial parts fraction.

No	Rt (minute)	Name	Molecular formula	MS and MS-MS	Group	A	B	C	D
1	0.9468	Homovanillyl alcohol	$C_9H_{12}O_3$	$[M-H]^+$ 169.0363	Phenolics			√	√
2	1.1019	Chinensinaphthol	$C_{22}H_{18}O_7$	$[M-H]^+$ 116.0705	Lignans			√	√
3	1.1973	Justicidone	$C_{20}H_{12}O_7$	$[M-H]^+$ 365.1045	Lignans		√	√	√
4	1.1425	Coumarin	$C_9H_6O_2$	$[M-H]^+$ 147.0378 $[C_5H_5]^+$ 65.0393 $[C_7H_7]^+$ 91.0542 $[C_8H_7O]^+$ 119.049	Coumarins			√	
5	1.5067	Cinnamic acid	$C_9H_8O_2$	$[M-H]^+$ 149.0293	Phenolics		√		
6	1.7891	Brazoide C	$C_{18}H_{26}N_2O_9$	$[M-H]^+$ 415.1692	Alkaloids		√		
7	4.7389	(+)-Lyoniresinol	$C_{22}H_{28}O_8$	$[M-H]^+$ 421.1466	Lignans			√	
8	6.2850	(8S,9R,9aS,10aR)-5-Oxo-9-vinyl-1,2,3,8,9,9a,10,10aoctahydro-5H-imidazo[1,2-a] pyrano [4,3-d]	$C_{18}H_{26}N_2O_8$	$[M-H]^+$ 399.1745	Alkaloids			√	√

No	Rt (minute)	Name	Molecular formula	MS and MS-MS	Group	A	B	C	D
		pyridin-8-yl-alpha-D-glucopyranoside							
9	6.6963	Rapanone	$C_{19}H_{30}O_4$	$[M-H]^+$ 323.1622 $[C_{10}H_9O_3]^+$ 177.0537	Cuinons		√	√	
10	7.7125	Justridusamide A	$C_{17}H_{23}NO_8$	$[M-H]^+$ 370.1469 $[C_7H_8N]^+$ 106.0651 $[C_7H_{12}O_4]^+$ 160.0748 $[C_{11}H_{10}NO_2]^+$188.0706 $[C_{11}H_{12}NO_3]^+$ 206.0812	Nitrogenous compound		√		
11	8.7758	(-)-Genpenterpene A	$C_{12}H_{16}O_3$	$[M-H]^+$ 209.0983	Terpenoids		√		
12	9.1025	1-Deoxy-1-{methyl[(2-oxo-2,3,4,5-tetrahydro-1H-1-benzazepin-7-yl) carbonyl] amino}hexitol	$C_{18}H_{26}N_2O_7$	$[M-H]^+$ 383.1876 $[C_4H_6NO]^+$ 84.0445 $[C_7H_8N]^+$ 106.0951 $[C_{10}H_{10}N]^+$ 144.0810 $[C_{12}H_{13}N_2O_2]^+$ 217.0979 $[C_{12}H_{15}N_2O_3]^+$ 235.1079	Alkaloids		√	√	
13	9.1026	5H,6H-quinindolin-11-one	$C_{15}H_{10}N_2O$	$[M-H]^+$ 235.0940 $[C_7H_8N]^+$ 106.0650 $[C_8H_8N]^+$ 118.0655 $[C_9H_8N]^+$ 130.0648 $[C_{11}H_{11}N_2]^+$ 171.0922	Alkaloids			√	
14	9.3644	Castanospermine	$C_8H_{15}NO_4$	$[M-H]^+$ 190.0753	Alkaloids		√		
15	9.4008	6-C-glusosyl-8-C-arabinosyl apigenin atau Schaftoside	$C_{26}H_{28}O_{14}$	$[M-H]^+$ 535.1411	Flavonoids		√	√	

No	Rt (minute)	Name	Molecular formula	MS and MS-MS	Group	A	B	C	D
16	10.2375	Gendarusin A	$C_{25}H_{26}O_{13}$	$[M-H]^+$ 535.1431 $[C_7H_5O_2]^+$ 121.0281 $[C_{17}H_{11}O_5]^+$ 295.0608 $[C_{18}H_{13}O_6]^+$ 325.0720 $[C_{21}H_{17}O_8]^+$ 397.0936 $[C_{18}H_{27}O_2]^+$ 499.1240	Flavonoids		√	√	
17	10.5596	3,4-Dihydroxy-6-(N-ethylamino) benzamide	$C_9H_{12}N_2O_3$	$[M-H]^+$ 197.1004	Phenolics		√		
18	10.8853	Gendarusin B	$C_{25}H_{26}O_{13}$	$[M-H]^+$ 535.1403 $[C_7H_5O_2]^+$ 121.0283 $[C_{14}H_{15}O_7]^+$ 295.0820 $[C_{18}H_{13}O_6]^+$ 325.0724 $[C_{25}H_{23}O_{11}]^+$ 499.1245	Flavonoids		√	√	
19	11.6129	6-{[(Benzyloxy) carbonyl]amino}-6-deoxy-1,2-O-isopropylidene-alpha-D-glucofuranose	$C_{17}H_{23}NO_7$	$[M-H]^+$ 354.1511	Nitrogenous compound		√		
20	12.7150	Protocatechuic acid	$C_7H_6O_4$	$[M-H]^+$ 154.9929	Phenolics				√
21	14.0909	Flindersine	$C_{14}H_{13}NO_2$	$[M-H]^+$ 228.1047	Alkaloids	√			
22	16.3481	Apigenin	$C_{15}H_{10}O_5$	$[M-H]^+$ 271.0777 $[C_5H_7]^+$ 67.0549 $[C_8H_7O]^+$ 119.0494 $[C_7H_5O_4]^+$ 153.0183	Flavonoids		√		
23	16.7338	Jaceosidin	$C_{17}H_{14}O_7$	$[M-H]^+$ 330.2986	Flavonoids		√		
24	16.7975	Chrysoeriol	$C_{16}H_{12}O_6$	$[M-H]^+$ 301.0743	Flavonoids		√		
25	20.6770	Savinin	$C_{20}H_{16}O_6$	$[M-H]^+$ 353.1135	Lignans	√			

No	Rt (minute)	Name	Molecular formula	MS and MS-MS	Group	A	B	C	D
26	20.8683	Sesamol	$C_7H_6O_3$	$[M-H]^+$ 139.0103	Phenolics		√		
27	21.5430	6-(2-Ethyl-5-hydroxy-hexoxy)-6-oxohexanoic acid	$C_{14}H_{26}O_5$	$[M-H]^+$ 275.1927	Fatty acids	√			
28	24.6151	(9Z)1,9-heptadecadiene-4, 6-diyne-3,8,11-triol	$C_{17}H_{24}O_3$	$[M-H]^+$ 277.2155 $[C_5H_7]^+$ 67.0545 $[C_6H_7]^+$ 79.0542	Fatty acids	√			
29	25.4601	12-Oxo-phytodienoic acid	$C_{18}H_{28}O_3$	$[M-H]^+$ 293.2000 $[C_4H_7]^+$ 55.0546 $[C_5H_7]^+$ 67.0545 $[C_{12}H_{15}]^+$ 159.1160 $[C_{18}H_{25}O]^+$ 257.1914 $[C_{18}H_{27}O_2]^+$ 275.1995	Fatty acids	√			
30	26.0763	Gamma-Linolenic acid	$C_{18}H_{30}O_2$	$[M-H]^+$ 279.2274 $[C_4H_7]^+$ 55.0546 $[C_5H_7]^+$ 67.0544 $[C_6H_9]^+$ 81.0705 $[C_7H_{11}]^+$ 95.0854 $[C_8H_{13}]^+$ 109.1006 $[C_9H_{15}]^+$ 123.1167 $[C_{13}H_{21}O_2]^+$ 209.1523 $[C_{14}H_{23}O_2]^+$ 223.1680 $[C_{18}H_{29}O]^+$ 261.2198	Fatty acids	√			
31	26.6814	9-OxoODE	$C_{18}H_{30}O_3$	$[M-H]^+$ 295.2051 $[C_4H_7]^+$ 55.0546 $[C_5H_7]^+$ 67.0545 $[C_5H_5O]^+$ 81.0699 $[C_{10}H_{15}O]^+$ 151.1111 $[C_{12}H_{17}]^+$ 161.1322	Fatty acids	√			

No	Rt (minute)	Name	Molecular formula	MS and MS-MS	Group	A	B	C	D
				$[C_{13}H_{19}O_2]^+$ 207.1364					
32	27.4184	5-Hydroxy-7,8-dimethoxy flavanone	$C_{17}H_{16}O_5$	$[C_{17}H_{27}]^+$ 231.2117 $[C_{18}H_{27}O]^+$ 259.2058 $[C_{18}H_{29}O_2]^+$ 277.2152 $[M-H]^+$ 301.1457	Flavonoids	√			
33	27.7739	13(S)-HODE	$C_{18}H_{32}O_3$	$[M-H]^+$ 297.2426 $[C_6H_9]^+$ 81.07 $[C_7H_{11}]^+$ 95.0856 $[C_8H_{13}]^+$ 109.1009 $[C_8H_{13}O]^+$ 125.0962 $[C_{10}H_{15}]^+$ 135.1173 $[C_{18}H_{29}O]^+$ 261.2204 $[C_{18}H_{31}O_2]^+$ 279.2310	Fatty acids	√			
34	31.5955	Juniperic acid	$C_{16}H_{32}O_3$	$[M-H]^+$ 273.2534	Fatty acids	√			
35	31.6745	Stigmasterol	$C_{29}H_{48}O$	$[M-H]^+$ 413.3213 $[C_7H_{11}]^+$ 95.0859 $[C_{10}H_{13}]^+$ 133.1000 $[C_{12}H_{15}]^+$ 159.1169 $[C_{15}H_{19}]^+$ 199.1486	Steroids	√			
36	32.3087	Taraxasterol	$C_{30}H_{50}O$	$[M-H]^+$ 427.3765	Terpenoids	√			
37	32.7056	Phytol	$C_{20}H_{40}O$	$[M-H]^+$ 297.3145 $[C_4H_9]^+$ 57.0703 $[C_5H_9]^+$ 69.0704 $[C_6H_{11}]^+$ 83.0860 $[C_7H_{13}]^+$ 97.1017 $[C_9H_{17}]^+$ 125.1322 $[C_{10}H_{19}]^+$ 139.1497	Terpenoids	√			

Note: A = *n*-hexane fraction; B = ethyl acetate fraction; C = *n*-butanol fraction; D = water fraction

Table 2: Identified metabolites with negative ionization in *J. gendarussa*'s aerial parts fraction.

No	Rt (minute)	Name	Molecular formula	MS and MS-MS	Group	A	B	C	D
1	1.1531	Taiwanin E methyl ether	$C_{21}H_{14}O_7$	$[M-H]^-$ 377.0855	Lignans			√	√
2	1.1558	Medioresinol	$C_{21}H_{24}O_7$	$[M-H]^-$ 387.1146	Lignans		√	√	√
3	6.2852	(8S,9R,9aS, 10aR)-5-Oxo-9-vinyl-1,2,3,8,9,9a,10 ,10aoctahydro-5H-imidazo[1,2-a] pyrano [4,3-d] pyridin-8-alpha-D-glucopyranoside	$C_{18}H_{26}N_2O_8$	$[M-H]^-$ 397.1619	Alkaloids			√	
4	7.7093	Justridusamide A	$C_{17}H_{23}NO_8$	$[M-H]^-$ 368.1358 $[C_4H_5O_3]^-$101.0230 $[C_4H_7O_4]^-$ 119.0345 $[C_6H_{11}O_5]^-$ 163.0603 $[C_{11}H_{10}NO_3]^-$ 204.067 $[C_{11}H_{12}NO_4]^-$ 222.0756	Nitrogenous compound		√		
5	8.3808	(3S,5R,6R)-3-Allyl-3-[(S)-hydroxy(4-nitrophenyl) methyl]-5,6-dimethoxy-5,6-dimethyl-1,4-380,1339dioxan-2-one	$C_{18}H_{23}NO_8$	$[M-H]^-$ 380.1381	Nitrogenous compound			√	
6	9.1028	1-Deoxy-1-{methyl[(2-oxo-2,3,4,5-tetrahydro-1H-1- benzazepin-7-yl) carbonyl] amino}hexitol	$C_{18}H_{26}N_2O_7$	$[M-H]^-$ 381.1668	Alkaloids			√	
7	9.1482	6-C-glusosyl-8-C-arabinosyl apigenin or Schaftoside	$C_{26}H_{28}O_{14}$	$[M-H]^-$ 563.1406	Flavonoids		√	√	
8	10.2012	Gendarusin A	$C_{25}H_{26}O_{13}$	$[M-H]^-$ 533.1308	Flavonoids		√	√	

No	Rt (minute)	Name	Molecular formula	MS and MS-MS	Group	A	B	C	D
9	10.8793	Gendarusin B	$C_{25}H_{26}O_{13}$	$[M-H]^-$ 533.1306	Flavonoids		√	√	
10	11.5937	Sesamol	$C_7H_6O_3$	$[M-H]^-$ 137.0402 $[C_6H_5O]^-$ 93.0336	Phenolics		√		
11	11.6158	6-{[(Benzyloxy) carbonyl]amino} -6-deoxy-1,2-O-isopropylidene-alpha-D-glucofuranose	$C_{17}H_{23}NO_7$	$[M-H]^-$ 352.1414	Nitrogenous compound		√		
12	16.3587	Methyl 2-[cyclohex-2-en-1-yl(hydroxy) methyl]-3-hydroxy-4-(2-hydroxyethyl)-3-methyl-5-oxoprolinate	$C_{16}H_{25}NO_6$	$[M-H]^-$ 327.2150	Nitrogenous compound		√		
13	16.4997	Apigenin	$C_{15}H_{10}O_5$	$[M-H]^-$ 269.0524	Flavonoids		√		
14	16.7387	Jaceosidin	$C_{17}H_{14}O_7$	$[M-H]^-$ 329.0441	Flavonoids		√		
15	16.8444	Chrysoeriol	$C_{16}H_{12}O_6$	$[M-H]^-$ 299.0760	Flavonoids		√		
16	22.0038	Gamma-Linolenic acid	$C_{18}H_{30}O_2$	$[M+H]^-$ 277.1847	Fatty acids	√			
17	24.6149	(-)-Secoisolariciresinol	$C_{20}H_{26}O_6$	$[M-H]^-$ 361.2199 $[C_6H_7O]^-$ 95.0488 $[C_7H_9O]^-$ 109.0655 $[C_9H_{15}O_3]^-$ 171.1023 $[C_{12}H_{19}O_3]^-$ 211.1335 $[C_{15}H_{18}O_3]^-$ 246.1255	Lignans	√			
18	25.9558	13(S)-HODE	$C_{18}H_{32}O_3$	$[M-H]^-$ 295.2273 $[C_7H_{13}O]^-$ 113.0963 $[C_{12}H_{19}O_2]^-$ 195.1383	Fatty acids	√			
19	26.2882	9-OxoODE	$C_{18}H_{30}O_3$	$[M-H]^-$ 293.1852 $[C_2H_3O_2]^-$ 59.0129 $[C_7H_{13}O]^-$ 113.0964 $[C_{10}H_{15}O_2]^-$ 167.1065	Fatty acids	√			

No	Rt (minute)	Name	Molecular formula	MS and MS-MS	Group	A	B	C	D
				$[C_{10}H_{17}O_3]^-$ 185.1175 $[C_{17}H_{29}O]^-$ 249.2233					
20	29.7393	Juniperic acid	$C_{16}H_{32}O_3$	$[M-H]^-$ 271.2267 $[C_{15}H_{29}O]^-$ 225.2206	Fatty acids	√			
21	32.3554	Stigmasta-4,22-dien-3-one	$C_{29}H_{46}O$	$[M-H]^-$ 409.3041	Steroids	√			

Note: A = *n*-hexane fraction; B = ethyl acetate fraction; C = *n*-butanol fraction; D = water fraction

A fragmentation example of the major secondary metabolite found in *J. gendarussa* was taken, namely gendarusin A. Gendarusin A belong to flavonoid groups (Ratih *et al.* 2019). The resulting fragmentations of gendarusin A are $[C_7H_5O_2]^+$ (m/z 121.0281), $[C_{17}H_{11}O_5]^+$ (m/z 295.0608), $[C_{18}H_{13}O_6]^+$ (m/z 325.0720), $[C_{21}H_{17}O_8]^+$ (m/z 397.0936), and $[C_{18}H_{27}O_2]^+$ (m/z 499.1240) following previous research (Rahmah 2022). In general, the fragmentation characteristic of flavonoid release H_2O (Sheng *et al.* 2021). This compound got release two H_2O $[M+H-36]^+$ m/z 499.1240, then release $C_4H_7O_3$ $[M+H-102]^+$ m/z 397.0936. Also, research by Rahmah (2022) reported that fragmentation reaction of gendarusan A is release $C_8H_{16}O_8$ from $[M+H]^+$ 535.14349 → $[M+H-C_8H_{16}O_8]+H^+$ 295.06143, which release arabinose (Table 1).

Compounds identified in positive ionization mode include phenolics, flavonoids, lignans, coumarins, quinones, terpenoids, fatty acids, steroids, alkaloids, and nitrogenous compounds that are following the literature on *J. gendarussa* that have been collected previously (Table 1). There are five phenolics groups identified, including homovanillyl alcohol, protocatechuic acid, cinnamic acid, 3,4-dihydroxy-6-(N-ethylamino) benzamide, and sesamol (Calderon *et al.* 2012; Anigboro *et al.* 2020; Rafi *et al.* 2022; Wahyuni *et al.* 2020; Basit *et al.* 2022). Seven flavonoids have been identified, including gendarusin A, gendarusin B, 5-hydroxy-7,8-dimethoxy flavanone, jaceosidin, chrysoeriol, apigenin, and schaftoside (Kumar *et al.* 2018; Ratih *et al.* 2019; Rafi *et al.* 2022). Four lignan metabolites were identified, including chinensinaphthol, (+)-lyoniresinol, savinin, and justicidone (Perez *et al.* 2004; Bharathi *et al.* 2020; Liu *et al.* 2022). The basic structure of coumarins was identified in *J. gendarussa* (Cassola *et al.* 2019). The quinone group was identified as rapanone (Ratih *et al.* 2019). Three metabolites have been identified in the terpenoid group, including phytol, taraxasterol, and (-)-genpenterpene A (Odokwo & Onifade 2020; Wahyuni *et al.* 2020; Zhang *et al.* 2021b). Seven fatty acids were identified, including 6-(2-Ethyl-5-hydroxy-hexoxy)-6-oxohexanoic acid, (9Z)1,9-heptadecadiene-4,6-diyne-3,8,11-triol, 12-Oxo-phytodienoic acid, gamma-linolenic acid, 9-OxoODE, 13(S)-HODE, and juniperic acid (Calderon *et al.* 2012; Ratih *et al.* 2019).

Seven metabolites of alkaloids group have been identified, including flindersine, castanospermine, brazoide C, (8S,9R,9aS, 10aR)-5-Oxo-9-vinyl-1,2,3,8,9,9a,10,10aoctahydro-5H-imidazo[1,2-a] pyrano[4,3-d] pyridin-8-yl-alpha-D-glucopyranoside, justridusamide A, 5H,6H-quinindolin-11-one, and 1-Deoxy-1-{methyl[(2-oxo-2,3,4,5-tetrahydro-1H-1-benzazepine-7-yl) carbonyl] amino}hexitol (Kiren *et al.* 2014; Indrayoni *et al.* 2016; Souza *et al.* 2017; Ratih *et al.* 2019; Zhang *et al.* 2021a; Basit *et al.* 2022). Apart from that, a steroid class metabolite was identified, namely stigmasterol (Uddin *et al.* 2011). Finally, nitrogenous compound that was identified was 6-{[(benzyloxy)carbonyl]amino}-6-deoxy-1,2-O-isopropylidene-alpha-D-glucofuranose (Ratih *et al.* 2019).

Compounds identified in negative ionization mode include phenolics, flavonoids, lignans, fatty acids, alkaloids, steroids and nitrogenous compounds (Table 2). The phenolic group identified was sesamol (Basit *et al.* 2022). Six flavonoid metabolites were identified, including gendarusin A, gendarusin B, apigenin, jaceosidin, chryosoeriol and schaftoside (Kumar *et al.* 2018; Ratih *et al.* 2019; Rafi *et al.* 2022). Three lignan metabolites were identified, including taiwanin E methyl ether, medioresinol, and (-)-secoisolariciresinol (Xu *et al.* 2019). Four fatty acid metabolites were identified, namely gamma-linolenic acid, 13(S)-HODE, juniperic acid, and 9-oxoODE (Ratih *et al.* 2019). The alkaloids identified were two metabolites, including (8S,9R,9aS, 10aR)-5-oxo-9-vinyl-1,2,3,8,9,9a,10,10aoctahydro-5H-imidazo[1,2-a]pyrano[4,3-d]pyridin-8-yl-alpha-D-glucopyranoside, and 1-deoxy-1-{methyl[(2-oxo-2,3,4,5-tetrahydro-1H-1 - benzazepine-7-yl) carbonyl] amino}hexitol (Souza *et al.* 2016; Ratih *et al.* 2019). In addition, a class of steroids was identified, namely stigmasta-4,22-dien-3-one (Uddin *et al.* 2011). Finally, four nitrogenous metabolites were identified, such as justridusamide A, (3S,5R,6R)-3-Allyl-3-[(S)-hydroxy(4-nitrophenyl) methyl]-5,6-dimethoxy-5,6-dimethyl- 1,4-380,1339dioxan-2-one, methyl 2-[cyclohex-2-en-1-yl(hydroxy) methyl]-3-hydroxy-4-(2- hydroxyethyl)-3-methyl-5-oxoprolinate, and 6-{[(Benzyloxy)carbonyl]amino}-6-deoxy-1,2-O-isopropylidene-alpha-D-glucofuranose (Khoo *et al.* 2015; Indrayoni *et al.* 2016; Ratih *et al.* 2019).

Visualization of Metabolites Distribution in *J. gendarussa* Fractions

Before PCA was carried out, the chromatogram was first optimized with COW. Visually, the chromatograms can be differentiated by fractionation based on the different levels of solvent polarity (Figures 2a and 2b). However, PCA will be carried out to reduce the data so that the distribution of metabolites can be seen based on different polarities. The resulting score plot for positive ionization mode produces data diversity of both PCs values of 79.7% with a PC1 value of 57.8% and PC2 of 21.9% (Figure 3a). The values of the two PCs show good two-

dimensional visualization because the diversity values of PC1 and PC2 are greater than 70% (Maulana *et al.* 2022). This shows that 79.7% of the data variability can be explained by the peak intensity of *J. gendarussa*'s aerial parts fraction based on different polarities. Likewise, with the score plot from PCA resulting in negative ionization mode, the diversity of data from both PCs values is 77.2% with a PC1 value of 45.2% and PC2 of 32% (Figure 3c). Based on the two PCA visualizations (Figures 3a and 3c), the resulting metabolites from the fractions can be grouped into three large groups, namely polar, semipolar and non-polar metabolites.

Apart from the plot score, there is a Biplot, which combines the plot score and loading plot to see which of the retention time plays a role in sample separation in PCA (Maulana *et al.* 2022). Based on the biplots in Figure 3b and Figure 3d, information is obtained that the metabolite at a particular retention time in the plot, which points towards the solvent, is the retention time which plays a role in grouping data in PCA for that solvent. Based on the overall PCA visualization, it can be concluded that fractionation significantly influences the distribution of *J. gendarussa* metabolites.

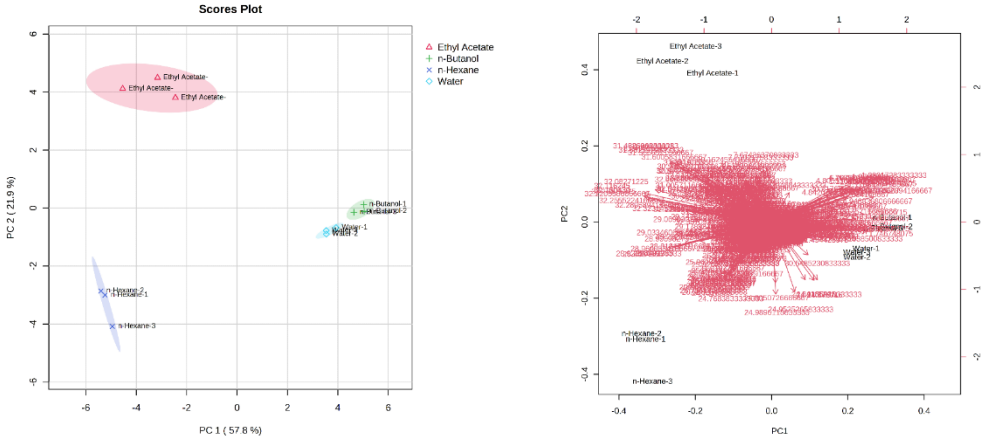

(a) (b)

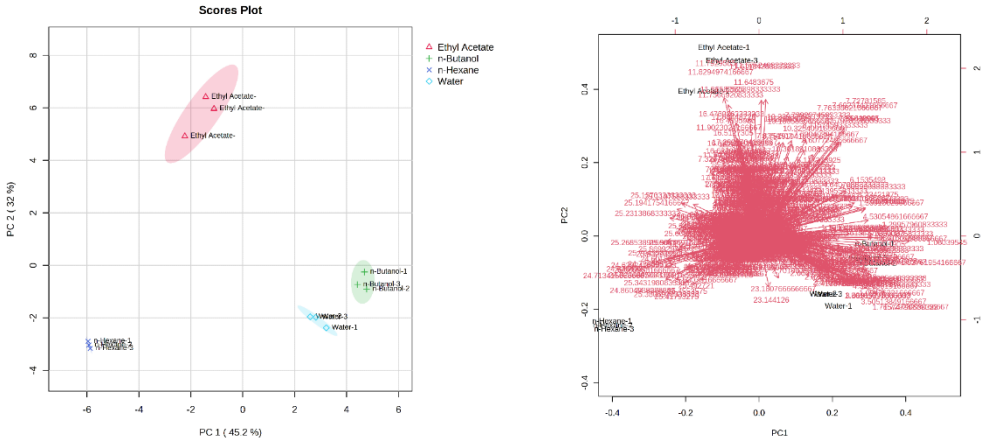

(c) (d)

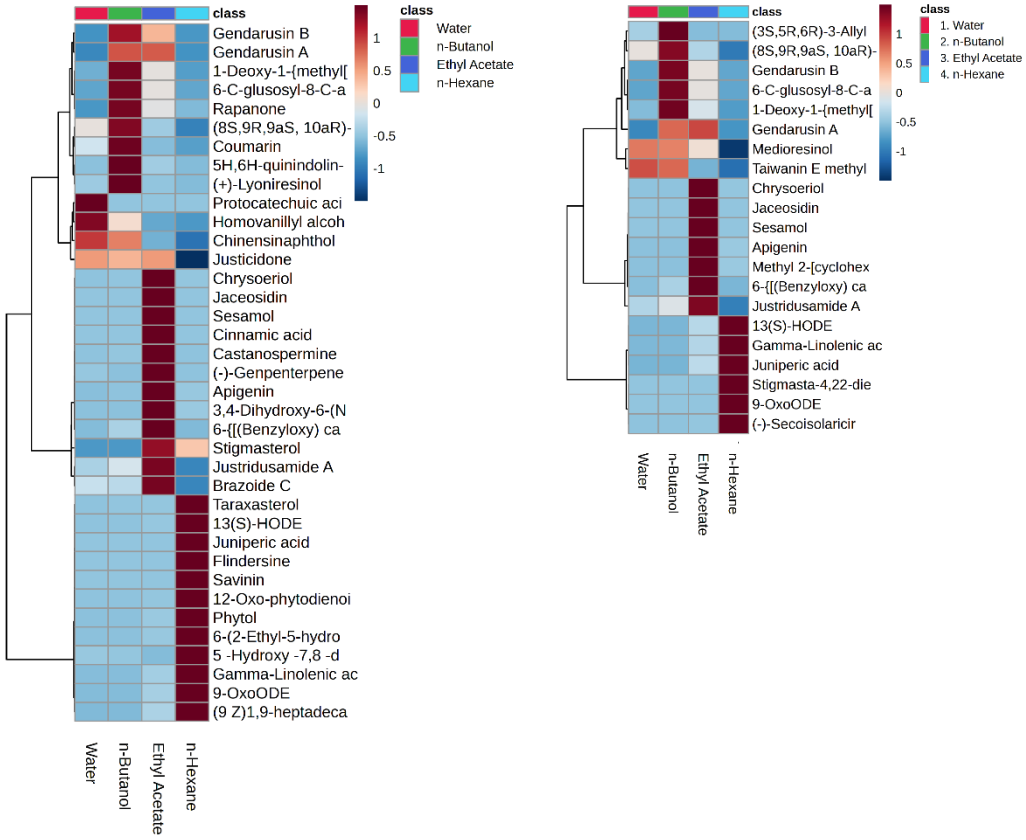

Fig. 3. PCA of *J. gendarussa* fraction (a) positive ionization plot score (b) positive ionization biplot (c) negative ionization plot score (d) negative ionization biplot. Heatmap of metabolites identified in *J. gendarussa*'s aerial parts fraction (e) positive ionization (f) negative ionization.

Furthermore, heatmap analysis will simplify the visualization of metabolite analysis so that it is easier to understand the separation of each metabolite that has been identified. This analysis can provide a more detailed understanding regarding the grouping of determining metabolites of each sample based on solvent polarity (Yuan *et al.* 2016). In addition, the resulting heatmap proves that metabolites with relatively high concentrations in a solvent are by the isolation of these metabolites in previous research (Figure 3e and 3f). Gendarusin A and B were isolated in the *n*-butanol fraction (Prajogo *et al.* 2009; Prajogo *et al.* 2016). Apigenin was successfully isolated in the ethyl acetate fraction (Kumar *et al.* 2018). Brazoide C was successfully isolated in the ethyl acetate fraction (Souza *et al.* 2016; Zhang *et al.* 2021a). Justridusamide A was isolated in the *n*-butanol fraction (Kiren *et al.* 2014). In addition, in the ethyl acetate fraction, (-)-genpenterpene A was successfully isolated (Zhang *et al.* 2021b).

The observed distribution of these metabolites is closely linked to their chemical structures and the principle of 'like dissolves like' across the solvent polarity gradient. The *n*-

hexane fraction primarily captured non-polar compounds, including fatty acids like gamma-linolenic acid and 9-OxoODE, as well as steroids such as stigmasterol. In contrast, the ethyl acetate and *n*-butanol fractions were rich in semipolar to polar compounds, specifically flavonoids (for example, gendarusin A, apigenin, and jaceosidin) and lignans (for example, savinin). The concentration of these phenolic-rich metabolites in the ethyl acetate and *n*-butanol fractions explains why these two fractions exhibited significantly higher antioxidant capacities in the DPPH, FRAP, and CUPRAC assays compared to the *n*-hexane and water fractions. Furthermore, the heatmap analysis (Figures 3e and 3f) reveals that although some major metabolites, such as gendarusin A, were present in both semipolar fractions, their relative abundances differed, suggesting that the synergistic effect of the specific metabolite matrix in each fraction plays a vital role in their overall biological potential.

Prediction of Potential Compounds as Antioxidant

OPLS-DA is a chemometric method used to explain variations between sample groups and eliminate data irrelevant to the information needed through orthogonalization. OPLS-DA can more easily exclude independent variables unrelated to classification and filter characteristic variables in the sample. OPLS-DA can also interpret models more quickly because it focuses on predictions, namely discriminants, that can be used in discriminant method to get the best classification results (Arendse *et al.* 2018).

The OPLS-DA model was evaluated using parameters consisting of cumulative values of R^2X, R^2Y, and Q^2. R^2X explains the variation of variable X, and R^2Y explains the variation of variable Y, which consists of predictive and orthogonal components. Q^2 shows the variation of Y predicted by model X in that component. The OPLS-DA model is said to have good predictive ability if it produces a Q^2 value > 0.5 (Zhang *et al.* 2019). These identified metabolites will be correlated with antioxidant capacity to predict the *J. gendarussa*'s active antioxidant compounds with OPLS-DA. All OPLS-DA models for DPPH, ABTS, FRAP, and CUPRAC produce Q^2 values > 0.5, meaning the resulting prediction models are good. Example the resulting OPLS-DA models of DPPH are shown in Figure 4a and 4b.

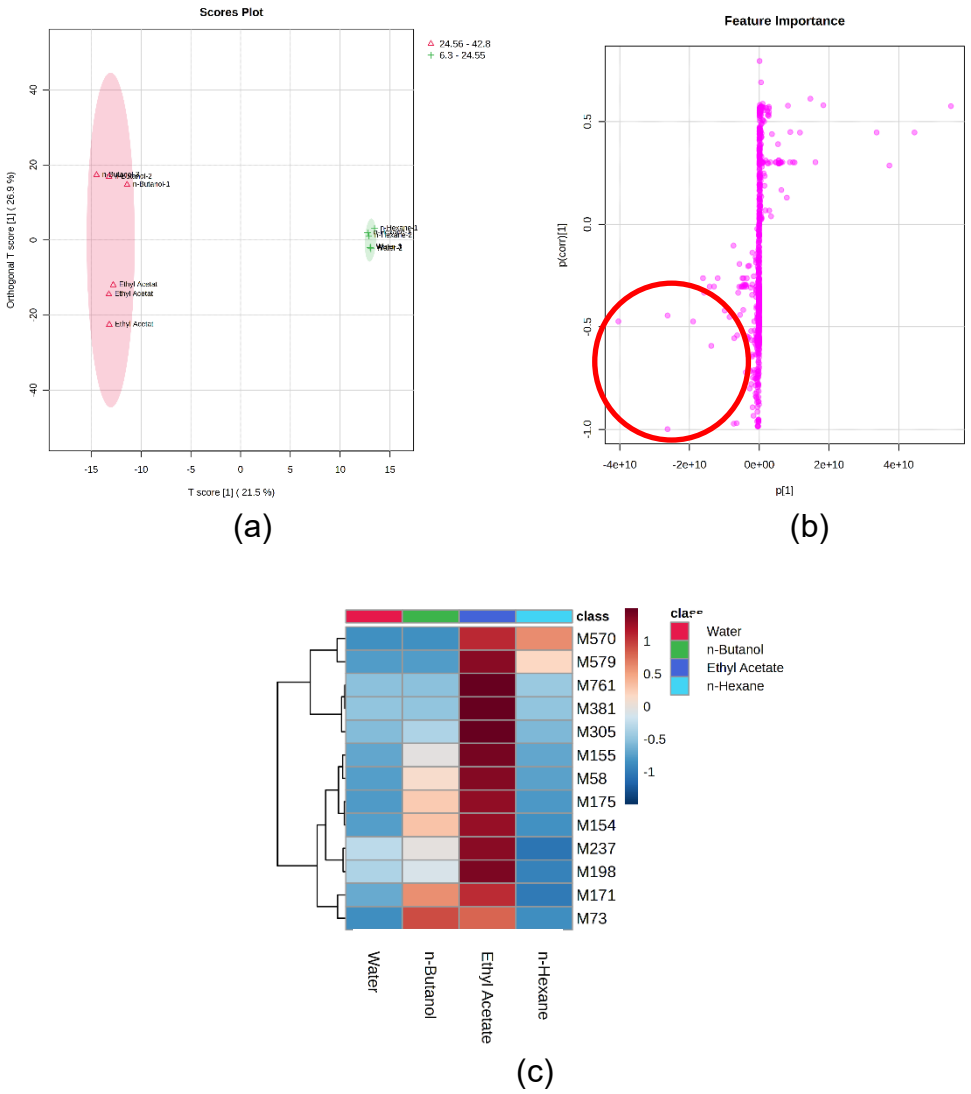

Figure 4. OPLS-DA of (a) DPPH method score plot (b) DPPH method S-plot (c) Heatmap of unknown compounds predicted as active antioxidant.

OPLS-DA was created using peak area variables from all m/z detected for identified and unknown metabolites and antioxidant capacity values. The antioxidant capacity value is classified by creating an interval between the lowest and the highest antioxidant capacity value (Tunnisa *et al.* 2022). The OPLS-DA score plot showed that the two groups were separated based on their antioxidant capacity. Example on DPPH method, the left quadrant shows the active group with high antioxidant capacity values consisting of the ethyl acetate and *n*-butanol fractions. In contrast, the right quadrant consists of the inactive *n*-hexane and water fractions with low antioxidant capacity values (Figure 4a). The score plot also shows that the model succeeded in grouping samples based on their antioxidant capacity.

Compounds that have the potential as antioxidants are predicted using S-plot. S-plot, the X-axis represents the variables contribution to the variance of the observed samples, while the Y-axis represents the correlation between samples and the results reliability (Xu *et al.* 2021). A combination of S-plot and several variables determines the compounds with the most probability act as an antioxidant. Variables were selected based on several criteria, namely p-value < 0.05, fold change > 2, and VIP > 1. VIP reflects the loading weight for each molecular weight variable and the response variability described by this value. Fold change is a measure that describes the change in quantity between the original measurement and the subsequent measurement (Luo *et al.* 2023). Based on these criteria, the predicted antioxidant active compounds will be in the lower left or upper right quadrant, fulfilling all the criteria. The plot score shows that the left quadrant is the group with high antioxidant capacity values, so that in the S-plot the lower left quadrant is the predicted area for active antioxidant compounds (Figure 4b). A summary of the active compound prediction results is attached in Table 3.

Table 3: Summary of predicted active antioxidant compounds with OPLS-DA.

Antioxidant method	Metabolites code	ESI	Metabolite name	Molecular weight	VIP value	Fold change
DPPH, ABTS, dan CUPRAC	M73	+	Unknown	123.0431	2.15	1201.40
	M745	-	Gendarusin A	533.1308	2.08	19.27
	M277	+	Gendarusin A	535.1431	2.09	18.66
	M171	+	Unknown	376.1307	2.01	9.97
	M154	+	Unknown	376.1258	1.92	32.21
	M58	+	Unknown	136.0552	1.80	82.31
	M175	+	Unknown	336.1271	1.77	196.84
FRAP	M381	+	Unknown	110.0242	1.26	435.24
	M440	+	Sesamol	139.0103	1.34	382.53
	M579	+	Unknown	609.2669	1.36	6.66
	M289	+	3,4-Dihydroxy-6-(N-ethylamino) benzamide	197.1004	1.69	6.28
	M783	-	Methyl 2-[cyclohex-2-en-1-yl(hydroxy) methyl]-3-hydroxy-4-(2-hydroxyethyl)-3-methyl-5-oxoprolinate	327.2150	1.64	90.12
	M715	-	Justridusamide A	368.1351	1.54	4.30
	M756	-	6-{[(Benzyloxy) carbonyl]amino} -6-deoxy-1,2-O-	352.1414	1.41	9.38

			isopropylidene-alpha-D-glucofuranose			
	M202	+	Justridusamide A	370.1469	1.55	5.15
	M761	-	Unknown	187.1061	1.69	71.82
	M305	+	Unknown	206.0759	1.65	23.08
	M198	+	Unknown	206.0786	1.54	4.65
	M302	+	6-{[(Benzyloxy) carbonyl]amino} -6-deoxy-1,2-O-isopropylidene-alpha-D-glucofuranose	354.1511	1.66	29.32
	M753	-	Sesamol	137.0402	1.68	249.66
	M155	+	Unknown	336.1272	1.53	9.42
	M570	+	Unknown	609.2676	1.18	3.96
	M154	+	Unknown	376.1258	1.44	5.06
	M237	+	Unknown	206.0769	1.46	3.91

Based on this table, gendarusin A and five unknown compounds were found as the predicted active antioxidant compounds using the DPPH, ABTS and CUPRAC methods. Then, using the FRAP method, 3,4-dihydroxy-6-(N-ethylamino) benzamide, 6-{[(Benzyloxy)carbonyl]amino}-6-deoxy-1,2-O-isopropylidene-alpha-D- glucofuranose, methyl 2-[cyclohex-2-en-1-yl(hydroxy) methyl]-3-hydroxy-4-(2-hydroxyethyl)-3-methyl-5-oxoprolinate, sesamol, and justridusamide A as well as nine unknown compounds as the predicted active antioxidant compounds. There were six identified metabolites and 14 unknown predicted as the active antioxidant compounds.

Each antioxidant method has its unique reaction. The FRAP method produces different results, which several factors can cause. FRAP obtains different results due to non-specific reactions to non-antioxidant compounds (Sadowska-Bartosz & Bartosz 2022). Then, the FRAP method reacts to a pH of 3.6, which is less representative of the biological situation, while the DPPH, ABTS, and CUPRAC methods have a reaction pH of 7.0 (Sadeer *et al.* 2020). Apart from that, the FRAP method also reacts weakly with flavonoid compounds. Therefore, gendarusin A is not predicted to be active in the FRAP method (Sadeer *et al.* 2020).

Unknown compounds identified as active antioxidants have the potential to be isolated and might be new chemical structure compounds to be obtained. Therefore, heatmap analysis was carried out specifically for the unknown compounds shown in Figure 4c. This was done to identify potential fractions for isolation in further research. Based on the heatmap (Figure 4c), the ethyl acetate fraction is dominant for isolation due to the high relative concentration of unknown compounds predicted to be active antioxidants. The six metabolites that have been

identified in *J. gendarussa* will be subjected to a DFT study to prove and strengthen the predicted results are active antioxidant compounds.

Density Functional Theory (DFT) of J. gendarussa Active Antioxidant Compounds

Computational chemistry methods for drug development are commonly used as a complement to *in vitro* and *in vivo* by medicinal chemistry researchers in exploring and finding lead compounds and modifying them into drug candidates (Salman *et al.* 2021). One approach that can be used to evaluate the ability of a compound as an antioxidant is density functional theory (DFT) studies. DFT is a highly accurate computational chemistry method that can provide detailed information about molecular properties, including reactivity and thermodynamics. One of the main properties obtained from DFT calculations is the system total energy, which is often called single point energy. Single point energy calculations provide insight into the stability, reactivity, and various properties of molecules. The highest occupied molecular orbital (HOMO) and lowest unoccupied molecular orbital (LUMO) energy values are the parameters used in this research (Kaddouri 2020).

The HOMO energy represents the highest energy level occupied by an electron in a molecule. A lower HOMO energy indicates a greater electron availability, making it more reactive in nucleophilic reactions. LUMO energy represents the lowest unoccupied energy level in a molecule, indicating its ability to accept electrons. A high LUMO energy indicates a good electron acceptor and tends to be more reactive in electrophilic reactions. Based on HOMO and LUMO energy, the ionization energy and electron affinity of a molecule can be calculated. Ionization energy is the amount of energy required to release one outermost electron from an atom. The smaller the ionization energy value, the easier it is for electrons to escape or move out of the path, so the molecule is said to be more reactive. Electron affinity is the energy change that occurs when an atom or molecule gains electrons. Higher electron affinity tends to make molecules more reactive (Azuxetullative 2020; Rammohan *et al.* 2020). The conclusion is that the best compound as an antioxidant is taken from the smallest energy gap (Islam 2015).

The energy gap is defined as the difference between the HOMO and LUMO energy values. The smaller the energy gap, the easier it is for electrons to be excited and the easier it is for a molecule to react. This is related to the antioxidant mechanism of the DPPH, ABTS, FRAP, and CUPRAC methods. A small energy gap characterizes compounds that are reactive to radicals, indicating good antioxidant activity (Sidiq 2021).

Table 4 summarizes all DFT results. Based on this table, the smallest ionization energy, largest electron affinity and smallest gap energy parameters are found in the compound 6-{[(Benzyloxy) carbonyl]amino}-6-deoxy-1,2-O-isopropylidene-alpha-D-

glucofuranose. The order of compounds based on the highest antioxidant power are 6-{[(Benzyloxy) carbonyl]amino}-6-deoxy-1,2-O-isopropylidene-alpha-D-glucofuranose > gendarusin A > trolox > 3,4-Dihydroxy-6- (N-ethylamino) benzamide > justridusamide A > sesamol > Methyl 2-[cyclohex-2-en-1-yl(hydroxy) methyl]-3-hydroxy-4-(2-hydroxyethyl)-3-methyl-5-oxoprolinate. Research by Srisayam *et al*. (2014), prove that sesamol has and IC_{50} value of 14.48 µM throught DPPH method. This proves that the prediction of active antioxidant compounds using OPLS-DA succeeded in obtaining two compounds with an energy gap smaller than the standard used to determine antioxidant capacity *in vitro*. Furthermore, isolation can be carried out to prove its antioxidant ability using metabolomics and density functional theory approaches.

Table 4: DFT active antioxidant compounds and trolox

Compound name	I (eV)	A (eV)	Molecular orbital
6-{[(Benzyloxy) carbonyl]amino}-6-deoxy-1,2-O-isopropylidene-alpha-D-glucofuranose	5.8635	3.4885	LUMO -3.4885 eV 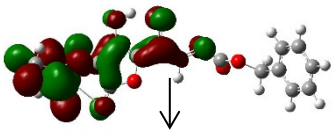 Energy gap (ΔE = 2.3750 eV) 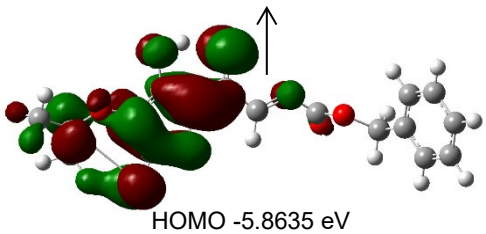 HOMO -5.8635 eV
3,4-Dihydroxy-6-(N-ethylamino) benzamide	5.9552	1.101	LUMO -1.101 eV 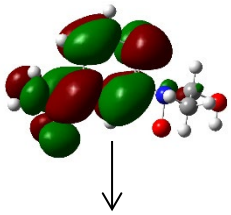 Energy gap (ΔE = 4.854 eV) 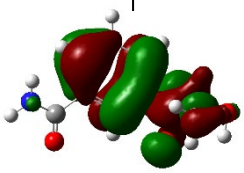 HOMO -5.9552 eV

Compound name	I (eV)	A (eV)	Molecular orbital
Gendarusin A	6.2409	2.160	LUMO -2.160 eV 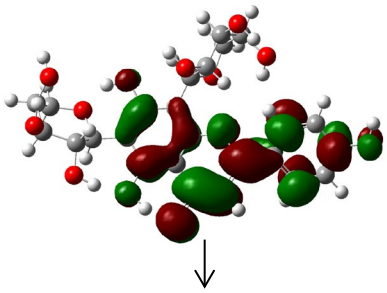 Energy gap (ΔE = 4.080 eV) 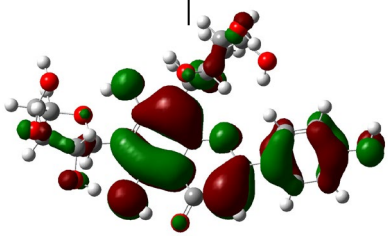 HOMO -6.2409 eV
Justridusamide A	6.0711	0.8775	LUMO -0.8775 eV 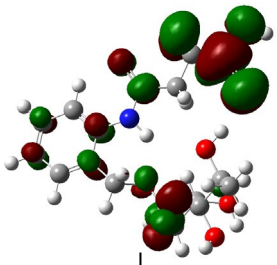 Energy gap (ΔE = 5.1936 eV) 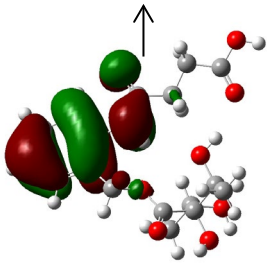 HOMO -6.0711 eV

Compound name	I (eV)	A (eV)	Molecular orbital
Methyl 2-[cyclohex-2-en-1-yl(hydroxy) methyl]-3-hydroxy-4-(2-hydroxyethyl)-3-methyl-5-oxoprolinate	6.3427	0.3695	LUMO -0.3695 eV 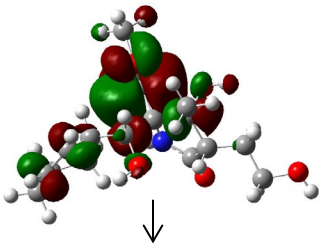 Energy gap (ΔE = 5.973 eV) 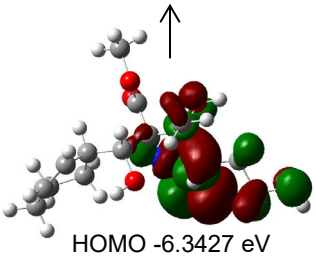 HOMO -6.3427 eV
Sesamol	5.5508	0.124	LUMO -0.124 eV 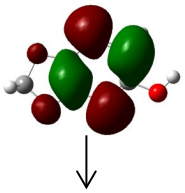 Energy gap (ΔE = 5.426 eV) 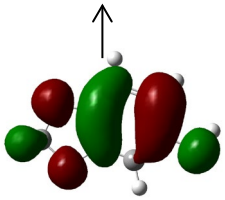 HOMO -5.5508 eV

Compound name	I (eV)	A (eV)	Molecular orbital
Trolox	5.2139	0.4481	LUMO -0.4481 eV 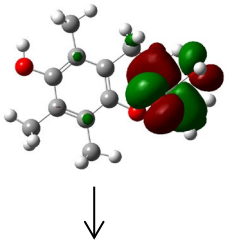 Energy gap (ΔE = 4.7658 eV) 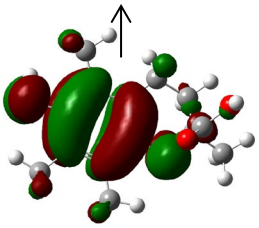 HOMO -5.2139 eV

CONCLUSION

The ethyl acetate and *n*-butanol fractions are the fractions that have the highest antioxidant capacity in the DPPH, ABTS, FRAP, and CUPRAC methods. There were 37 and 21 metabolites identified in positive and negative ionization using UHPLC-Q-Orbitrap HRMS, respectively. PCA and heatmap succeeded in differentiating metabolites based on polarity. OPLS-DA succeeded in identifying six active metabolites and 14 unknown compounds that had the potential to be isolated in the ethyl acetate fraction. The DFT study proves that the best antioxidant compound is 6-{[(benzyloxy) carbonyl]amino}-6-deoxy-1,2-O-isopropylidene-alpha-D-glucofuranose and gendarusin A compared trolox as a standard. Therefore, those two compounds are the best antioxidant compounds.

CONFLICT OF INTERESTS

The authors declare that they have no conflict of interest.

ETHICAL GUIDELINES DECLARATION

The authors declare that they have meet the research ethical guidelines.

ACKNOWLEDGEMENTS

This work was funded by Dexa Group through Dexa Award Science Scholarship.

AUTHORS' CONTRIBUTIONS

F.M. contributed in conceptualization, resources, methodology, data analysis, writing – original draft.
W.N., T., and I.B., contributes in supervision, methodology, and writing – review and editing.

All authors read and approved the final manuscript.

REFERENCES

Anigboro A A, Avwioroko O J, Ohwokevwo O A, Pessu B and Tonukari N J. (2020). Phytochemical profile, antioxidant, α-amylase inhibition, binding interaction and docking studies of Justicia carnea bioactive compounds with α-amylase. *Biophysical Chemistry* 269, 106529.

Arendse E, Fawole O A, Magwaza L S, Nieuwoudt H and Opara U L. (2018). Evaluation of biochemical markers associated with the development of husk scald and the use of diffuse reflectance NIR spectroscopy to predict husk scald in pomegranate fruit. *Scientia Horticulturae* 232: 240–249. Doi:org/10.1016/j.scienta.2018.01.022.

Azuxetullatif, Emriadi, Syukri and Putri U. (2020). Mempelajari senyawa mirisitrin dengan penambahan substituent NH_2, NO_2, dan CH_3 sebagai inhibitor korosi menggunakan metode density functional theory (DFT). *Chempublish Journal* 5(2): 166-178. doi: 10.22437/chp.v5i2.11347.

Basit A, Ahmad S, Khanan K U R, Sherif A E, Aati Y H, Ovatlarnporn C, Khan M A *et al.* (2022). New mechanistic insights on *Justicia vahlii* Roth: UPLC-Q-TOF-MS and GC-MS based metabolomics, in vivo, in-silico toxicological, antioxidant based anti-inflammatory and enzyme inhibition evaluation. *Arabian Journal of Chemistry* 15(10): 1-22.

Batubara I, Komariah K, Sandrawati A and Nurcholis W. (2020). Genotype selection for phytochemical content and pharmacological activities in ethanol extracts of fifteen types of *Orthosiphon aristatus* (Blume) Miq. leaves using chemometric analysis. *Sci Rep* 10(1): 1–11. doi:10.1038/s41598-020-77991-2.

Bharathi D, Subbiah L, Thangavelu P and Palanisamy S. (2020). Assessment of anti-psoriatic activity of ethanolic extract of *Justicia tranquebariensis* Linn. on amelioration of IMQ-induced hyperkeratosis in Balb/C mice. *Journal of Applied Pharmaceutical Sciences* 10(12): 83-89.

Calderón A I, Hodel A, Wolfender J L, Gupta M P, Correa M and Hostettmann K. (2012). LC–DAD–MS-based metabolite profiling of three species of Justicia (Acanthaceae). *Natural Product Research* 27(15): 1335-1342. doi: 10.1080/14786419.2012.738207.

Çalişkan B, Çalişkan A C, Çalişkan B and Çalişkan A C. (2021). Antioxidant and Oxidative Stress. IntechOpen. [download on 2023 Sept 16]. Available at: https://www.intechopen.com/chapters/75568.

Cassola F, Silva R H M, Borghi A A, Lusa G M, Sawaya F H C A, Garcia L V and Mayer S L J. (2019). Morphoanatomical characteristics, chemical profiles, and antioxidant activity of three species of *Justicia* L. (Acanthaceae) under different growth conditions. *Instrial Corps & Products* 131(2019): 257-265.

Chaudhary S. (2015). Evaluation of antioxidant and anticancer activity of extract and fractions of *nardostachys jatamansi* DC in breast carcinoma. *BMC complementary and Alternative Medicine* 50(2015): 1-13.

Di Meo S and Venditti P. (2020). Evolution of the knowledge of free radicals and other oxidants. *Oxid. Med. Cell. Longev* 2020: 9829176. doi:10.1155/2020/9829176.

Heryanto R, Putra C A, Khalil M, Rafi M, Putri S P, Karomah A H and Batubara I. (2023). Antioxidant activity and metabolite profiling of *Xylocarpus granatum* exctracts using gas chromatography-mass spectrometry. *Metabolites* 13(156): 1-13.

Indrayoni P, Purwanti D I, Wongso S, Prajogo B E W and Indrayanto G. (2016). Metabolite profiles in various plant organs of *Justicia gendarussa* Burm.f. and its in vitro cultures. *Sci. Pharm* 84: 555-566.

Islam N. (2015). Investigation of comparative shielding of Morin against oxidative damage by radicals: a DFT study. *Cogent Chem* 1(1): 2-9.

Kaddouri Y, Abrigach F, Yousfi E, Kodadi M E and Touzani R. (2020). New thiazole, pyridine and pyrazole derivatives as antioxidant candidates: synthesis, DFT calculations and molecular docking study. *Heliyon* 6. doi: 10.1016/j.heliyon.2020.e03185.

Khoo L W, Mediani A, Zolkeflee N K Z, Leong S W, Ismail I S, Khatib A, Shaari K and Abas F. (2015). Phytochemical diversity of *Clinacanthus nutans* extracts and their bioactivity correlations elucidated by NMR based metabolomics. *Phytochemistry Letters* 14: 123-133.

Kiren Y, Deguchi J, Hirasawa Y, Morita H and Prajogo B. (2014). Justidrusamides A-D, new 2-aminobenzyl alcohol derivatives from *Justicia gendarussa*. *J Nat Med* 68(4): 754-758.

Kuber R. (2021). In vitro antioxidant potential, total phenolic and flavonoid contents in *Justicia gendarussa* leaf extracts. *Res J Pharm Technol* 14: 2707–2713. https://doi.org/10.52711/0974-360X.2021.00477.

Kumar K S, Sabu V, Sindhu G, Rauf A A and Helen A. (2018). Isolation, identification and characterization of apigenin from *Justicia gendarussa* and its anti-inflammatory activity. *Int Immunopharmacol* 59(2018): 157–167. doi:10.1016/j.intimp.2018.04.004.

Liu B, Zhang T, Xie Z, Hong Z, Lu Y, Long Y, Ji C, Liu Y, Yang Y and Wu H. (2022). Effective components and mechanism analysis of anti-platelet aggregation effect of *Justicia procumbens* L. *Journal of Ethnopharmacology* 294(10).

Luo Z, Liu L, Nie Q, Huang M, Luo C, Sun Y, Ma Y, Yu J and Du F. (2023). HPLC-based metabolomics of *Dendrobium officinale* revealing its antioxidant ability. *Frontiers in Plant Sciences* 14(1060242): 1-13.

Maulana F, Muhammad A A, Umar A, Mahendra F R, Musthofa M and Nurcholis W. (2022). Profiling metabolites through chemometric analysis in *orthosiphon aristatus* extracts as α-glucosidase inhibitory activity and in silico molecular docking. *Indonesian Journal of Chemistry* 22(2): 501–514.

Nurcholis W, Alfadzrin R, Izzati N, Arianti R, Vinnai A B, Sabri F, Kristof E and Artika M I. (2022). Effects of methods and durations of exctraction on total flavonoid and phenolic contents and antioxidant activity of java cardamom (*Amomum compactum* soland ex maton) fruit. *Plants* 11(17): 1-13.

Odokwo E O and Onifade M S. (2020). Volatile constituents of the leaves and stem of *Justicia secunda* Vahl. *Communication in Physical Sciences* 6(2): 827-834.

Perez A J, Boluda C, Lopez H and Trujillo M J. (2004). Justicidone, a novel p-quinone-lignan derivative from *Justicia hyssopifolia*. *Chem Pharm Bull* 52(1): 1-130.

Prajogo B, Guliet D, Queiroz F, Wolfender J, Cholies N, Aucky H and Hostettmann K. (2009). Isolation of male antifertility compound in n-butanol fraction of *justicia gendarussa burm. f.* leaves. *Folia Medica Indonesiana* 45(1): 28-31.

Prajogo B, Widyanti P and Riza H. (2016). Effect of free alkaloid and non-free alkaloid ethanol 70% exctract of *Justicia gendarussa burm f* againsts reverse transcriptase HIV enzyme in vitro and chemical compound analysis. *Indonesian Journal of Tropical and Infectious Disease* 6(1): 1-4.

Putri V A Z, Asra R and Chandra B. (2020). Overview of phytochemical and pharmacological of gandarussa extract (*Justicia gendarussa Burm*). *EAS J Pharm Pharmacol* 2(5): 180–185. doi:10.36349/easjpp.2020.v02i05.003.

Rafi M, Karomah A H, Septaningsih D A, Rahminiwati M, Putri S P and Iswantini D. (2022). LC-MS/MS based metabolite profiling and lipase enzyme inhibitory activity of

Kaempferia angustifolia Rosc. with different extracting solvents. *Arabian Journal of Chemistry* 15(11): 104232.

Rahmah N N. (2022). Kajian metabolomik dan bioaktivitas ekstrak metanol daun gandarusa yang dibudidaya dengan kombinasi pupuk kandang dan NPK Master diss., IPB University.

Ramadhan R G, Imelda, Kusuma R T and Phameswari D S. (2021). Analisis aktivitas antioksidan dan sitotoksik senyawa pelargonidin sebagai kandidat obat menggunakan metode DFT (density functional theory). *Jurnal Kimia Saintek dan Pendidikan* 5(2): 110-120. e-ISSN: 2615-3378.

Rammohan A, Bhaskar V B, Jr A C, Gunasekar D, Gu W and Zyryanov G V. (2020). In silico, in vitro antioxidant and density functional theory based structure activity relationship studies of plant polyphenolics as prominent natural antioxidants. *Arabian Journal of Chemistry* 13(2): 3690-3701.

Ratih G A M, Imawati M F, Nugroho R R, Purwanti D I, Wongso S, Prajogo B and Indrayanto G. (2019). Phytochemicals of gandarusa (*Justicia gendarussa*) and its preparations. *Nat Prod Commun* 14(6): 1–10. doi:10.1177/1934578X19851406.

Sadeer B N, Montesano D, Albrizio S, Zengin G and Mahomoodally F M. (2020). The versatility of antioxidant assays in food science and safety-chemistry, application, strengths, and limitations. *Antioxidants* 9(709): 1-39.

Sadowska-Bartosz I and Bartosz G. (2022). Evaluation of the antioxidant capacity of food products: methods, applications and limitations. *Processes* 10(2031): 1–23. doi:10.3390/pr10102031.

Salman M, Al-Obaidi Z, Kitchen P, Loreto A, Bill R M and Wade R. (2021). Advances in applying computer-aided drug design for neurodegenerative diseases. *Int J Mol Sci* 22(9): 4688.

Sheng Z, Jiang Y, Liu J and Yang B. (2021). UHPLC-MS/MS analysis on flavonoids composition in astragalus membranaceus and their antioxidant activity. *Antioxidant* 10(11): 1-14. doi:10.3390/antiox10111852.

Sidiq R. (2021). Analisis Komputasi Inhibisi Korosi Besi oleh Senyawa Derivat Kuinolin Undergraduate diss., Universitas Andalas.

Souza G L, Almeida S C M, Lemos G L T, Ribeiro V R P, Canuto M K, Braz-Filho R, Cistia D N C, Anna S R M C, Barreto S F and Moraes O M. (2016). Brazoide A-D, new alkaloid from *Justicia gendarussa Burm.* F. species. *J Braz Chem Soc* 0(0): 1-7.

Srisayam M, Weerapreeyakul N, Barusrux S, Kanokmedhakul K. (2014). Antioxidant, antimelanogenic, and skin-protective effect of sesamol. *J Cosmet Sci*. 65:69-79

Tunnisa F, Faridah D N, Afriyant A, Rosalina D, Syabana M A, Darmawan N and Yuliana N D. (2022). Antioxidant and antidiabetic compunds identification in several indonesian

underutilize Zingiberaceae spices using SPME-GC-MS-based volatilomics and in silico methods. *Food Chemistry* 14(4): 1-10.

Uddin R M, Sinha S, Hossain A M, Kaisar A M, Hossain K M and Rashid A M. (2011). Chemical and biological investigations of *Justicia gendarussa* (Burm. f). *Dhaka Univ J Pharm Sci* 10(1): 53-57.

Wahyuni D K, Huda A, Faizah S, Purnobasuki H and Wardojo B P E. (2020). Effects of light, sucrose concentration and repetitive subculture on callus growth and medically important production in *Justicia gendarussa Burm*.f. *Biotechnol Reports* 27: e00473. doi:10.1016/j.btre.2020.e00473.

Widodo A, Khumaidi A and A Lasongke P F. (2019). Toksisitas ekstrak etanol dan ekstrak air dari daun jotang kuda (*Synedrella nodiflora* (L.) Gaertn.), daun gandarusa (*Justicia gendarussa Burm*.F.), dan daun pulutan (*Urena lobata* L.) dengan brine shrimp lethality test. *J Farm Galen (Galenika J Pharmacy)* 5(2): 198–205. doi:10.22487/j24428744.2019.v5.i2.13935.

Xu C, Liang L, Yang T, Feng L, Mao X and Wang Y. (2021). In-vitro bioactivity evaluation and non-targeted metabolomic analysis of green tea processed from different tea shoot maturity. LWT. *Food Sci. Technol* 152: 1-9. doi:10.1016/j.lwt.2021.112234.

Xu X, Wang D, Ku C, Zhao Y, Cheng H, Liu K, Rong Li and Zhang H. (2019). Anti-HIV lignans from *Justica procumbens*. *Chin J Nat Med* 17(12): 945-952.

Yuan J, Murphy A, Koeyer D D, Lague M and Bizimungu B. (2016). Effectiveness of the field selection parameters on potato yield in Atlantic Canada. *Can J Plant Sci* 96: 701-710.

Zhang H, Xia Z, Xu T, Chen Y and Zhou G. (2021a). New compounds from the aerial parts of *Justicia gendarussa Burm f* and their antioxidant and anti-inflammatory activities. *Natural Product Research* 35(20): 3478-3486.

Zhang H, Xia Z, Xu T, Xu W, Chen Y and Zhou G. (2021b). One pair of new enantiomeric trinorsesquiterpenes from the aerial parts of *Justicia gendarussa*. *Natural Product Research* 23(12): 1140-1147.

Zhang Y, Yu P and Liu P. (2019). Using high-throughput metabolomics to discover perturbed metabolic pathways and biomarkers of allergic rhinitis as potential targets to reveal the effects and mechanism of geniposide. *RSC Adv* 9: 17490–17500. doi: 10.1039/c9ra02166c.